CHARACTERIZATION OF MULLITE-ZIRCONIA COMPOSITES PREPARED FROM VARIOUS STARTING ALUMINA PHASES

H. Belhouchet[1], V. Garnier[2]

(1) Département de Physique, Faculté des Sciences, Université de M'Sila, 28000 (Algérie)

(2) INSA de Lyon, laboratoire MATEIS UMR CNRS 5510, Bât. Blaise Pascal, 7 Av. Jean Capelle, 69621 Villeurbanne (France)

E-mail: hbelhou@yahoo.com

Abstract

Zirconia-dispersed mullite composites were prepared by reaction sintering of boehmite, γ-alumina, ($\delta+\theta$)-alumina and α-alumina as sources, mixed with zircon powder. The powder mixtures were ball-milled and isostatically pressed into disks. The obtained samples were sintered between 1400 and 1600°C for 2h in air. The resulting sintered materials were characterized in terms of bulk density, dilatometry, DTA/TG, XRD and SEM. From the dilatometric and differential thermal analysis curves, several microstructural transformations which occur in these samples are detailed in this work. XRD peaks suggested fully developed mullite and zirconia phases by reaction sintering of zircon and all alumina phases. Zircon usually dissociates at temperature higher than 1665°C. However, it is shown in this study that zircon dissociates at about 1400°C due to the presence of transition alumina phases. The microstructure of all the composites is composed of irregularly shaped mullite grains, and round-shaped zirconia grains which are distributed intragranularly and intergranularly.

Résumé

Des composites à dispersoïdes mullite-zircone ont été préparés par frittage réactif de : la boehmite, l'alumine-γ, l'alumine-($\delta+\theta$) et l'alumine-α comme sources de départ, mélangé avec la poudre de zircon. Les mélanges des poudres ont été soumis à un broyage à boulets, puis pressés isostatiquement sous forme de disques, enfin frittés entre 1400 et 1600°C sous air pendant 2h. Ces céramiques ont été étudiées à travers la densité, la dilatométrie, l'analyse thermique différentielle et thermogravimétrique, la diffraction des rayons X et la microscopie électronique à balayage. À partir des courbes dilatométriques et d'analyse thermique différentielle, nous avons constaté que plusieurs transformations microstructurales se sont produites. Les spectres de diffraction des rayons X ont mis en évidence la formation des composites mullite-zircone à partir de zircon et des différentes phases d'alumine de départ. Le zircon se dissocie normalement à une température élevée (1665°C), cependant, dans notre cas nous avons montré que la dissociation a lieu à une température plus basse (1400°C). Ce décalage est causé par la présence des phases d'alumine de transition. La microstructure des échantillons préparés est composée de gros grains de mullite, de forme irrégulière et de grains de zircone de forme grossièrement arrondie, distribués d'une manière homogène dans la matrice mullitique (inter/intragranulaire).

Mots clés: Mullite-zirconia; composites; Reaction sintering; Zircon; Alumina phases

1- INTRODUCTION

Mullite has excellent potential candidate for high-temperature engineering materials because of its low thermal expansion coefficient, low thermal conductivity, high temperature strength, high creep resistance, and phase stability up to the melting point [1]. However, monolithic mullite ceramics exhibit both low strength and fracture toughness at room temperature [2-5]. It is therefore necessary to use reinforced mullite ceramics for practical applications [6]. Reinforcing mullite has been produced by incorporating second-phase particles such as zirconia (ZrO_2). In particular, the addition of ZrO_2 promotes densification and retards grain growth of mullite phase in mullite-zirconia composites [7]. The mechanical properties of sintered in situ reacted mullite-zirconia composites were accordingly investigated. Microcrack toughening is assumed to be the predominant mechanism for the high toughness and strength found for these bodies [8-13].

Various processing routes for preparing mullite-zirconia composites have been reported [1] including: (1) sintering of mixed mullite and ZrO_2 powders, (2) reaction sintering of alumina, silica and zirconia, and (3) reaction sintering of alumina and zircon. From these preparation methods, the reaction sintering is the most common one because of its advantages to use cheap commercial raw materials and low processing cost. However, the process is difficult to control due to the simultaneous occurrence of densification and reaction [9-10, 14].

The aim of the present study is to prepare mullite-zirconia composites from reaction sintering of zircon and four different alumina sources (boehmite, γ-Al_2O_3, $(\delta+\theta)$-Al_2O_3 and α-Al_2O_3). Microstructural studies on the samples sintered at 1600°C have been carried out. To understand the formation of the mullite-zirconia composite, thermal and physical characterizations were also performed.

2- PROCEDURE EXPERIMENTALE

The following powders were used as starting materials:

(1) Boehmite (AlOOH), γ-Al_2O_3, $(\delta+\theta)$-Al_2O_3 and α-Al_2O_3 obtained from partial and complete dehydration of a gibbsite (supplied by Diprochim, Algerian company) were used as the alumina sources. The average particle size of the gibbsite powder is 75 µm.

(2) Fine zircon ($ZrSiO_4$) powder (supplied by Moulin des près, France company) with 1.5 µm average grain size (given by the producer).

The chemical composition of the starting materials is listed in Table 1. The samples were prepared to obtain a 3:2 molar ratio for Al_2O_3:SiO_2 with the mixture of boehmite+zircon, γ-alumina+zircon, $(\delta+\theta)$-alumina+zircon and α-alumina+zircon, they are named BZ, GZ, DTZ and AZ respectively. All the sources of alumina powders were attrition milled with alumina balls in aqueous media for 3 h to reduce d_{50} to 1.5 µm. Milling was carried out under the following conditions: the powder to ball ratio was kept to 1:10 by weight, the addition of approximately 0.25 wt. % of ammonium polymethacrylate dispersant (Darvan C) and ammoniac was used to adjust the pH of the suspensions to 10.4. Homogenization of the mixtures of alumina and zircon was achieved by ball-milling for 20 h in distilled water using alumina balls in diameter of 1.5-2 mm and a plastic container under the same preceding dispersion conditions.

After milling, the mixtures were dried at 110°C and 1 wt. % polyvinyl alcohol (PVA) + 0.5 wt. % polyethylene glycol (PEG) were added as binder by mortar mixing, then the mixtures were granulated through a 45 µm sieve. The samples were uniaxially pressed at 7 MPa followed by cold isostatic pressing at 250 MPa as disks (diameter: 15 mm). Isopressed samples were heated up to 600°C at a rate of 1°C/min to burn out the binder. To determine an optimum preliminary sintering temperature, the compacts were then sintered in air to temperatures in the range 1400-1600°C for 2 h soaking using a heating rate of 5°C/min.

Tableau 1: *Chemical analysis of raw materials (wt. %)*

| Elements	Boehmite	γ, $(\delta+\theta)$ and α-alumina	Zircon
LOI*	06	-	-
Al_2O_3	88.34	93.98	-
ZrO_2	-	-	63.50
SiO_2	3.86	4.10	35.50
F	0.90	0.96	-
Na_2O	0.34	0.36	-
CaO_2	0.18	0.19	-
Fe_2O_3	0.08	0.10	0.08
Ti_2O	-	-	0.10
HfO_2	-	-	1.50
K_2O	0.07	0.08	-

* LOI: Loss of Ignition.

Particle size distribution analysis was carried out for the different powders mixtures using a laser granulometey with a Mastersizer 2000 (Malvern Instruments). Powders were subjected to differential thermal analysis (DTA) and thermogravimetric analysis (TGA) using Setaram TAG 92 with α-alumina as the reference material at a heating rate of 5°C/min in air. The bulk density of the sintered composites was measured by water displacement method using Archimedes' principle. For thermal expansion measurement, 10 mm length and 10 mm diameter cylindrical rods were prepared. Linear thermal expansion was performed on the cylindrical rods using Setaram TMA 92 dilatometer up to 1600°C with 5°C/min heating rate. Phases of sintered composites were identified by X-ray diffraction using a Rigaku Cmax-I diffractometer [Ni-filtered $Cu_{k\alpha}$ X radiation (40kV-25mA) with a scanning speed of 2° (2θ) per minute and 0.05° of step. The areas of the peaks (111) and $(11\bar{1})$ of monoclinic zirconia, (111) of

tetragonal zirconia, (200) of zircon, (113) of α-alumina and (110) of mullite were used in the quantitative analysis. Fraction of dissociated zircon, mullite formation and bulk retained t-ZrO_2 were determined on the polished surface of as-sintered samples using the method proposed by Pena et al. [15]. A scanning electron microscope (SEM) was recorded from the polished surface of a thermally etched sample using SEM (JEOL-840-A).

3- RESULTS AND DISCUSSIONS

The chemical composition of the starting materials used in this study is presented in Table 1. It clearly shows that the content of impurity is high in all powders; the boehmite has a small loss during ignition due to the presence of structural water. The particle size distributions of the different powders mixtures are given in Fig. 1, measured by the particle size analyser after milling for 20 h. The average particle size (d_{50}) of all powders mixtures was ~ 0.2 µm.
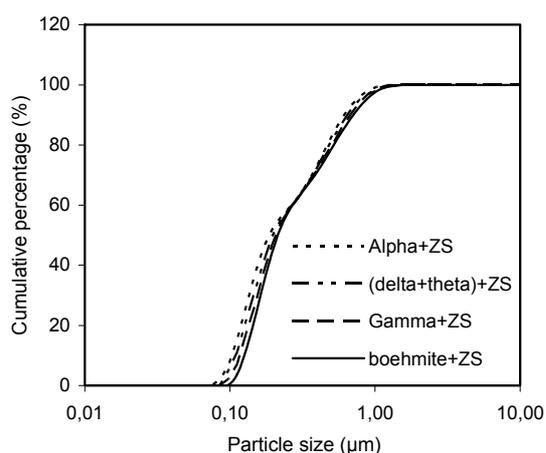
Fig. 1: *Particle size distribution of mixed powders after milling*

The results of thermogravimetric analysis of samples are given in Fig. 2. The weight loss in BZ mixture occurs in three stepped temperature. The first one located around 110°C is due to adsorbed water, the second (around 250°C) is correlated to the losses of structural water from gibbsite. Indeed, part of boehmite rehydrates and crystallizes to form the gibbsite (Al(OH)$_3$) during milling [16]. In Fig. 3, X-ray diffraction pattern of the powder mixture milled 20 h by ball milling confirms the boehmite rehydration and the formation of the gibbsite (Al(OH)$_3$) during milling [17]. The third step of the weight loss in BZ mixture (Fig. 2) around 460°C is due to evaporation of structural water in boehmite.

The TGA results of BZ mixture shows also that the total water loss is very high (≈ 11%). In the GZ mixture, the weight loss occurred in two stages; at 110°C and between 110 and 500°C. The weight loss at 110°C is due to adsorbed water. The weight loss between 110 and 500°C is due to evaporation of structural water introduced during milling and release of binder. The TGA curve of DTZ shows that the weight loss around 250 and 350°C is due to dehydration of structural water and release of binder. The TGA curve of AZ shows that the weight loss around 250 and 350°C is only due to release of binder (1.5 wt. %).
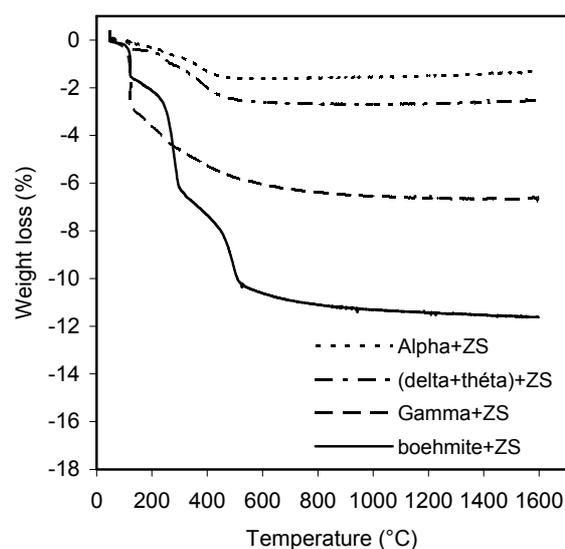

Fig. 2: *Thermogravimetric analysis of zircon + alumina mixtures*
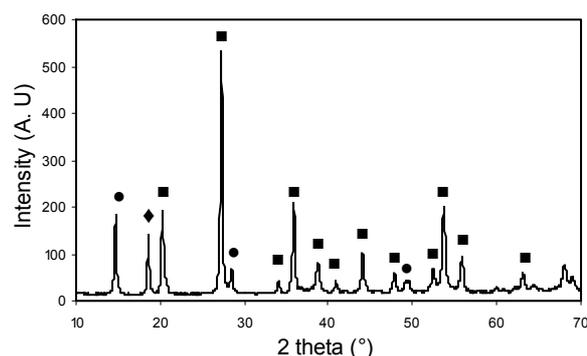
Fig. 3: *XRD patterns of the boehmite-zircon powder after 20 h for milling. (●: boehmite, ♦: gibbsite, ■: zircon)*

The differential thermal analysis of powders mixtures are shown in Fig. 4. The DTA curve of BZ mixture shows two successive endothermic peaks [18]. The first one around 290°C is due to the loss of structural water from the gibbsite formed

during milling and the second endothermic peak around 500°C is due to transformation of boehmite into γ-alumina [19]. A much smaller exothermic peak is hardly detected in all powders mixtures (except for α-Al$_2$O$_3$) around 1100-1200°C due to transformation of (δ+θ)-alumina to α-alumina. The DTA results for all powders mixtures show a similar sharp endothermic peak at 1500°C which is due to decomposition of zircon in zirconia and silica. XRD patterns confirm the reaction between α-alumina and silica to form the mullite-zirconia composite at 1500°C after 2 h of soaking (see Fig. 8).
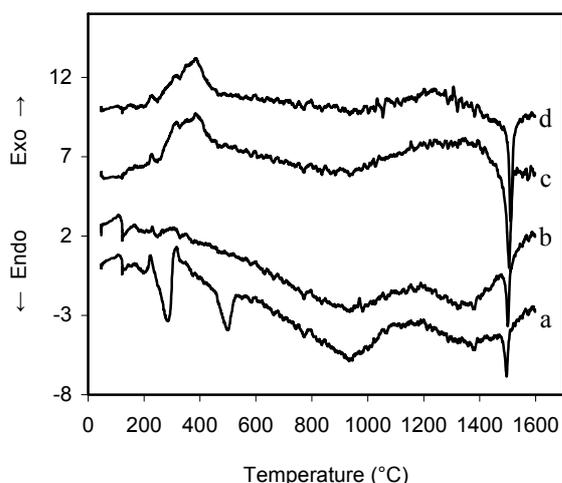
Fig. 4: *DTA of zircon + alumina mixtures. (a: boehmite+ZS; b: gamma+ZS; c: (delta+theta)+ZS; d: Alpha+ZS)*

The dilatometric curves shown in Fig. 5 were recorded for all the different samples using the following heat treatment cycle: heating from room temperature up to 1600°C and cooling to room temperature. The heating rate was 5°C/min and the cooling rate was 20°C/min. The whole heat treatment cycle was performed under static atmosphere of air.

The samples shrinkage starts in all cases, at about 1000°C, and may be related to the establishment of necks between the particles and/or to rearrangement between the particles and/or to the density variation occurring during alumina transformation. The curve recorded with the mixture BZ shows an expansion of the sample at about 1340°C. Similar expansions have been observed during sintering of GZ and DTZ samples, wich is not the case for AZ (Fig. 5). This expansion is probably related to the beginning of the zircon decomposition in t-ZrO$_2$ and silica (vitreous phase) which should be caused by the transformation of a residual amount of θ phase toward α phase.
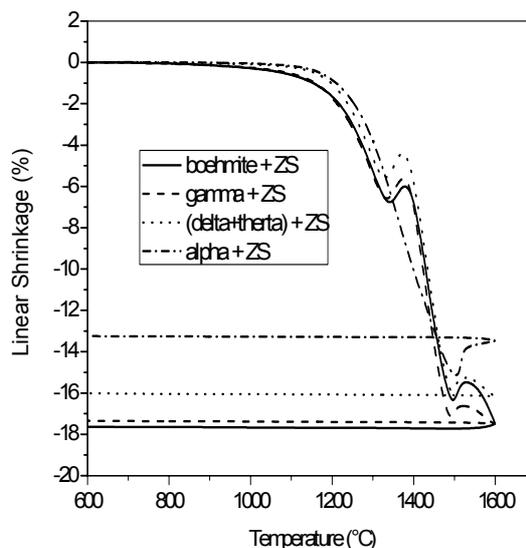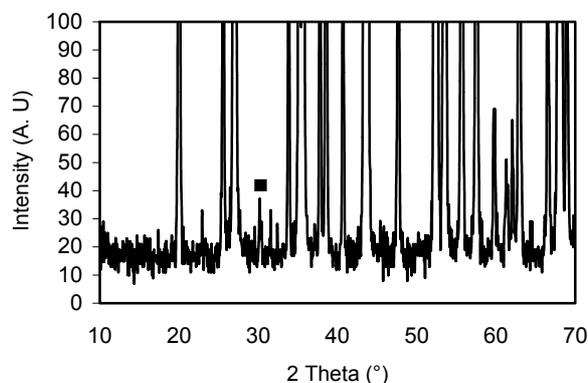

Fig. 5: *Dilatometric curves recorded from different samples during the sintering treatment*

Fig. 6 confirms the presence of residual θ phase at 1340°C and the absence of t-ZrO$_2$, but at 1385°C, Fig. 7 shows only α phase and t-ZrO$_2$ formation.
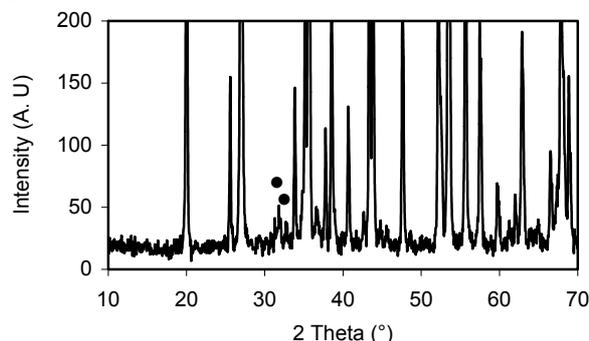

Fig. 6: *XRD patterns of the boehmite-zircon treated at 1340°C with the cooling rate were 100°C/min. (●:θ-alumina)*

Fig. 7: XRD patterns of the boehmite-zircon treated at 1385°C with the cooling rate were 100°C/min. (■: t-ZrO$_2$)

However after this expansion the shrinkage starts again with a larger rate in the cases of BZ, GZ and DTZ. Another expansion is observed on the dilatometric curves in all samples at 1500°C as a consequence of simultaneous ends of decomposition of zircon in zirconia and silica, and mullite-zirconia composite formation. Afterwards, the shrinkage starts again, at about 1540°C in cases of BZ, GZ and DTZ samples it is probably related to the elimination of residual porosity created by the transformation of θ phase toward α phase. For the AZ sample, we observed a continuous expansion up to 1600°C.

XRD patterns for samples of different alumina sources with zircon are given in Fig. 8. The ZrO_2 peaks can be observed in BZ, GZ and DTZ samples at a low temperature of ~ 1400°C; while at the same temperature no ZrO_2 peaks appear in the AZ sample.
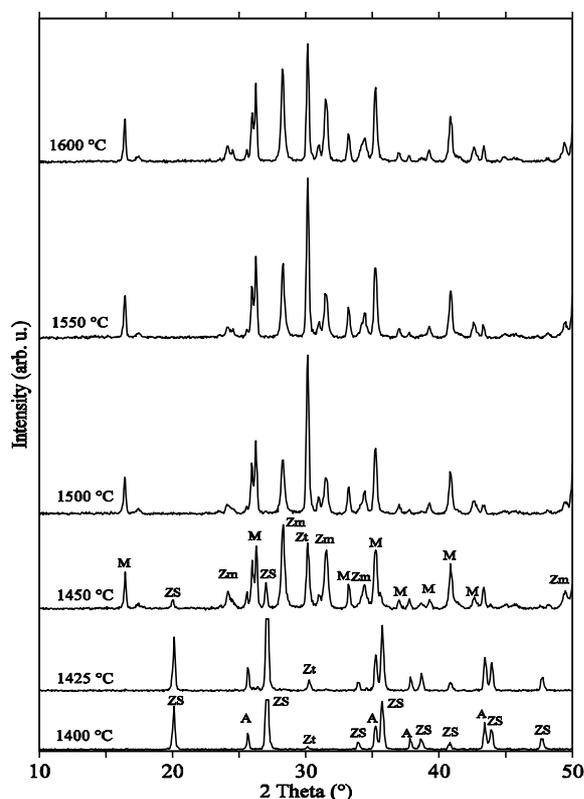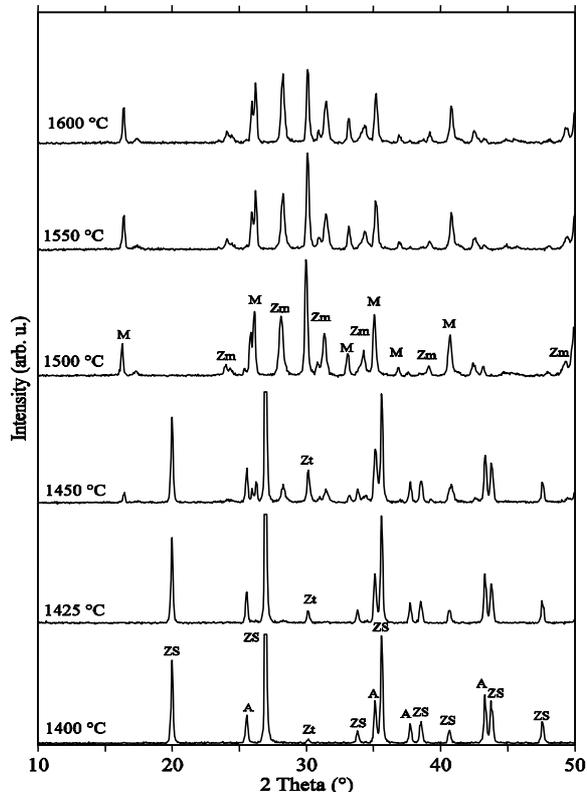

Fig. 8a: *XRD patterns of BZ samples treated at different temperature for 2 h. (ZS: zircon; A: α-alumina; M: mullite; Zm: monoclinic zirconia; Zt: tetragonal zirconia)*

As it is well known, pure zircon usually dissociates at a temperature higher than 1665°C [20]. But in the present study, zircon dissociation is initiated by the presence of transition alumina phases, and could take place at a lower temperature of 1400°C in BZ, GZ and DTZ samples.
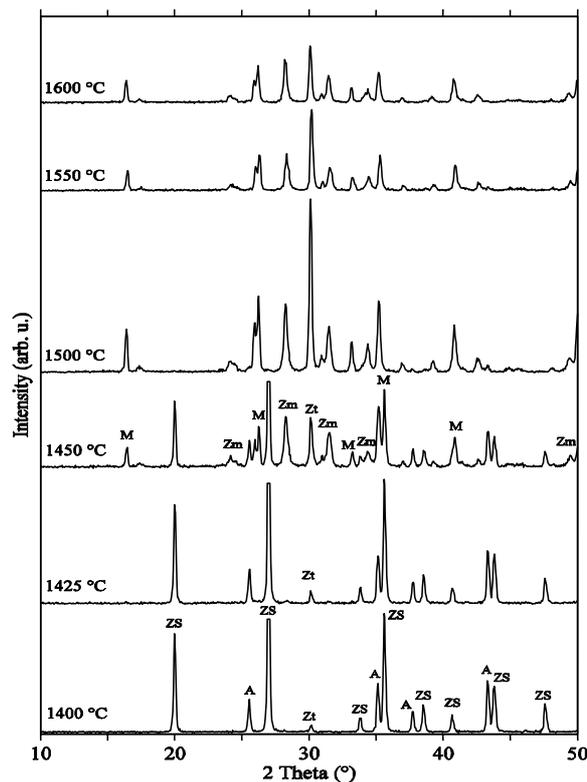
Fig. 8b: *XRD patterns of GZ samples treated at different temperature for 2 h. (ZS: zircon; A: α-alumin; M: mullite; Zm: monoclinic zirconia; Zt: tetragonal zirconia)*

Fig. 8c: *XRD patterns of DTZ samples treated at different temperature for 2 h. (ZS: zircon; A: α-alumina; M: mullite; Zm and Zt: monoclinic and tetragonal zirconia)*
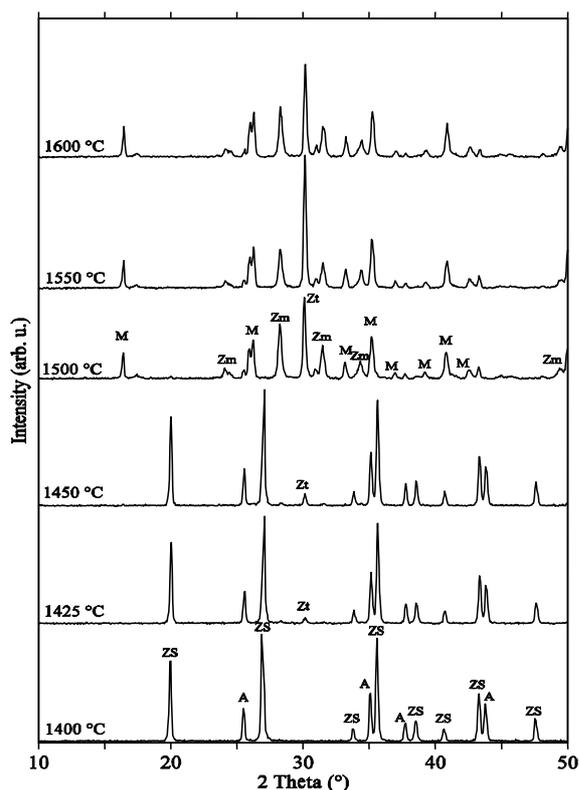
Fig. 8d*: XRD patterns of AZ samples treated at different temperature for 2 h. (ZS: zircon; A: α-alumina; M: mullite; Zm: monoclinic zirconia; Zt: tetragonal zirconia)*

In these three mixtures, BZ, GZ and DTZ are most reactive phases compared to the α-alumina phase. No crystalline SiO_2 peaks have been observed, which indicates the formation of amorphous SiO_2 phase.

With increasing the temperature to 1450°C, mullite peaks are observed in the BZ, GZ and DTZ samples with a great quantity in the case of BZ (75%, 50% and 30% in the BZ, GZ and DTZ respectively, see Fig. 9), while, for the AZ sample, mullite appears firstly at 1500°C, suggesting a better reactivity of boehmite, γ-alumina and (δ+θ)-alumina phases with zircon. This is consistent with the study of starting materials effect on the reaction sintering of mullite-zirconia composites by Ebadzadeh and Ghasmi [19].

The dissociation of zircon in BZ, GZ and DTZ samples is achieved at 1500°C (Fig. 10), while for the AZ sample it achieves at 1550°C. Fig. 11 reveals that at 1400°C the zirconia formed from dissociation of zircon is just tetragonal type in the BZ, GZ and DTZ samples, while in the case of AZ sample this dissociation occurs at 1425°C. Therefore, it seems likely, that the size of formed tetragonal particles at ~ 1400°C could be lower than the critical size for "t → m" transformation [10, 21].

Another factor should be also taken into account to understand the phase change of ZrO_2. It is well known that ZrO_2 phase transformation is related to a presence of SiO_2. At low temperature such as 1400°C, ZrO_2 and amorphous SiO_2 is formed due to $ZrSiO_4$ dissociation, and ZrO_2 particles is immersed in the amorphous SiO_2 matrix, which stabilizes ZrO_2 as t-ZrO_2 phase. At higher temperature, however, the amorphous SiO_2 is consumed to form mullite, losing the ability to stabilize ZrO_2; thus, the ZrO_2 in the samples obtained at higher temperature mainly exist in m-ZrO_2 phase [22].
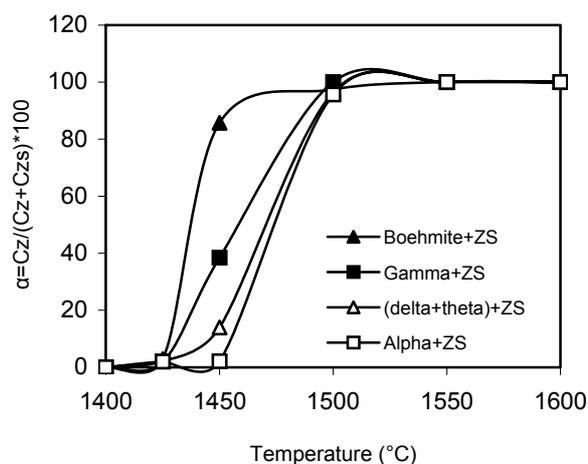

Fig. 9*: Zircon dissociation versus sintering temperature after 2 h heating. C_Z and C_{ZS}, the concentration of zirconia and zircon, respectively*
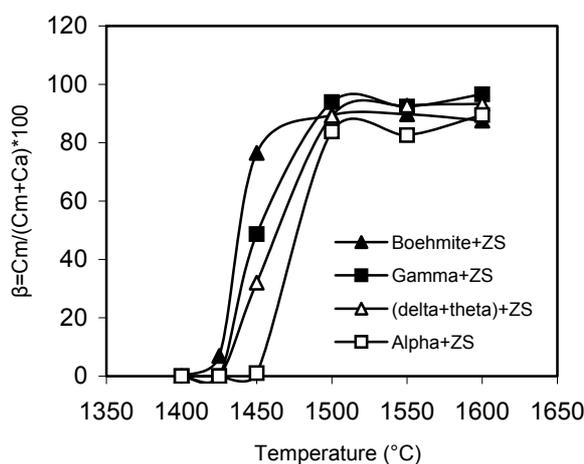

Fig. 10*: Mullite formation versus sintering temperature after 2 h heating. C_m and C_a, the concentration of mullite and alumina, respectively*

The bulk density of the samples sintered at various temperatures for 2 h are shown in Fig. 12. In all four samples, variations of the densification are similar. The zircon and α-alumina mixture is relatively dense at

21

1425°C in all samples between 3.1 and 3.6 g.cm^{-3}. The formation of mullite is responsible of the density decrease in BZ sample between 1425 and 1450°C; on the other hand for all the other samples density starts to decrease between 1450 and 1500°C, as confirmed by the enhancement of the mullite peaks intensity in the X-ray diffraction patterns. Thereafter, between 1500 and 1600°C the density increases in the same way for all the samples. The maximum density (3.65 g.cm^{-3}) has been observed for all samples at 1600°C.
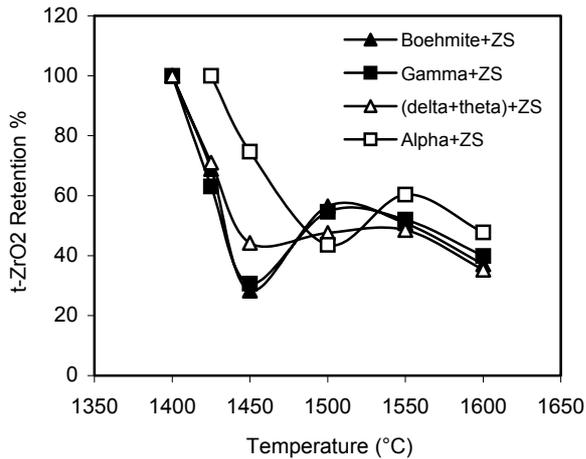

Fig. 11: *Tetragonal zirconia fraction in reaction sintering samples as a function of firing temperature (duration 2 h)*
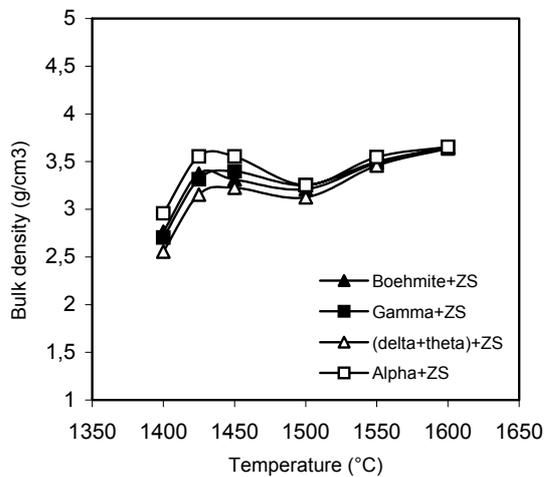

Fig. 12: *Bulk density of various samples as function of firing temperature (duration: 2 h)*

Fig. 13 shows the scanning electron microstructure of polished and thermally etched surface of four samples sintered at 1600°C for 2 h. As expected with the X ray analysis the microstructure of all samples shows a mullite-zirconia composite (two phase). We note a homogeneous microstructure with an uniformly distributed porosity. All samples are composed of irregularely large shaped mullite grains and

round shaped zirconia grains which are distributed both intergranularly and intragranularly. Intergranular zirconia (monoclinic phase) is localised especially in a triple points of the mullite/mullite particles or at the vicinity of the pores. Whereas the intragranular zirconia (tetragonal phase) with a lower size is practically present in all the mullite grains. Let us note, finally, that there is a higher porosity within these samples; the corresponding pores are localised in the grains boundaries. The ratio of intragranular zirconia grains is higher in the AZ samples than in the other samples.
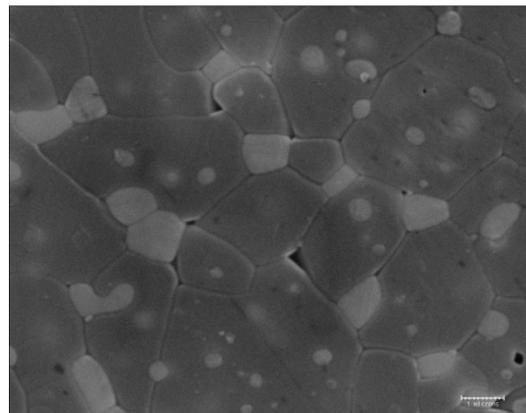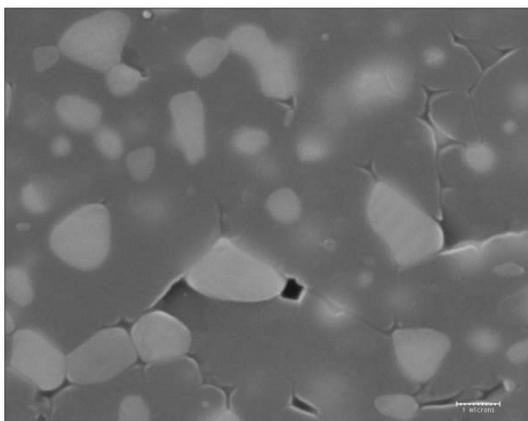

(a)
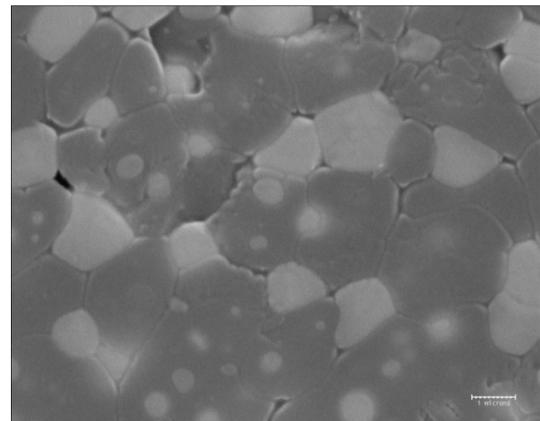
(b)
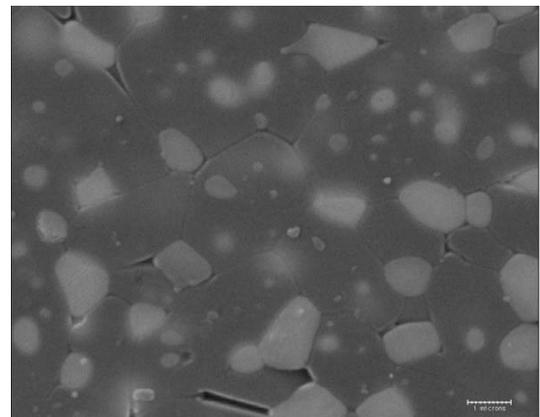
(c)

(d)

Fig. 13*: SEM photographs of polished and thermally etched surface of samples fired at 1600°C for 2 h. (a: Bohmite-zircon; b: γ-alumina-zircon; c: (δ+θ)-alumiba-zircon; d: α-alumina-zircon)*

4- CONCLUSION

We investigated mullite-zirconia composites prepared from zircon and different alumina sources. The DTA curves have shown endo and exothermic peaks, and dilatometric curves shown the presence of the expansions. The experimental results are summarized as follows:

(1) In the boehmite-zircon mixture, the particles of boehmite rehydrate and crystallize out of gibbsite $(Al(OH)_3)$ after the contact with the water during milling.

(2) The presence of tow expansions:
   - The first around 1340°C is due to the zircon decomposition in $t-ZrO_2$ and silica (vitreous phase) caused by the transformation of a residual quantity of θ phase toward α phase.
   - The second one around 1500°C is due to end of dissociation of zircon and mullitezirconia formation simultaneously.

(3) The total decomposition of zircon and the formation of mullite-zirconia achieved at 1500°C in the BZ, GZ and DTZ, while it achieves in the AZ sample at 1550°C.

(4) In all four samples, the densification varies in the same way, and we obtain the same higher value of density for all samples at 1600°C.

(5) In all samples, the microstructures are composed of irregularly mullite and intra/intergranularly dispersed zirconia grains.

REFERENCES

[1] H. Schneider, K. Okada, and J. A. Pask, Mullite and mullite ceramics, John wiley & Sons, Inc. New York, (1994)

[2] M. I. Osendi and C. Baudin, Mechanical properties of mullite materials, J. Eur. Ceram. Soc., Vol. 16, (1996), pp. 217-224

[3] P. Boch and T. Chartier, Tape casting and properties of mullite and zirconia-mullite ceramics, J. Am. Ceram. Soc., Vol. 74, N°91, (1991), pp. 2448-2452

[4] A. Grace, I. M. Low, G. R. Burton, T. Garrod, D. Zhou, R. D. Skala, D. N. Philips, and M. Pallai, Synthesis and properties of mullite ceramics derived from fumed silica and various amulinas, J. Mater. Sci. lett., Vol. 14, (1995), pp. 1310-1313

[5] M. Mizuno, Microstructure, Microchemistry, and flexural strength of mullite ceramics, J. Am. Ceram. Soc., Vol. 74, N°12, (1991), pp. 3017-3022

[6] K. S. Mazdiyasni, L. M. Brown, Synthesis and mechanical properties of stoichiometric aluminium, J. Am. Ceram. Soc., Vol. 55, (1972), pp. 548-552

[7] S. Prochazka, J. S. Wallace, and N. Claussen, Microstructure of sintered mullite–zirconia composites, J. Am. Ceram. Soc., Vol. 66, N°8, (1983), pp. C-125-C-127

[8] T. Koyama, S. Hayashi, A. Yasumori, K. Okada, M. Schmucker, and H. Schnieder, Microstructure and mechanical properties of mullite-zirconia composites prepared from alumina and zircon under various firing conditions, J. Eur. Ceram. Soc., Vol. 16, (1996), pp. 231-237.

[9] N. Claussen and J. Jahn, Mechanical properties of sintered, In-Situ reacted mullite–zirconia composites, J. Am. Ceram. Soc., Vol. 63, N°3-4, (1980), pp. 228-229

[10] J. S. Wallace, G. Petzow, and N. Claussen, Microstructure and property development in In Situ-reacted mullite-zirconia composites, Advances in Ceramics, Vol. 12, (1981), pp. 436-442

[11] R. Torrecillas, J. S. Moya, S. de Aza, H. Gros, and G. Fantozzi, Microstructure and mechanical properties of mullite–zirconia

reaction sintered composites, Acta Metall. Mater., Vol. 41, N°6, (1993), pp. 1647-1652

[12] J. S. Moya and M. I. Osendi, Microstructure and mechanical properties of mullite/ZrO_2 composites, J. Mater. Sci., Vol. 19, (1984), pp. 2909-2914

[13] Y. Yang, Z. Yang, and Q. Yuan, Al_2O_3 platelet and tetragonal zirconia particle incorporation reinforced mullite matrix ceramics, J. Mater. Sci. Lett., Vol. 15, (1996), pp. 185-186

[14] E. I. Di Rupo, M. R. Anseau, "Solid state reactions in the $ZrO_2 \cdot SiO_2$-Al_2O_3 system," J. Mater. Sci., Vol. 15, (1980), pp. 114-118

[15] P. Pena, P. Miranzo, J. S. Moya, S. De Aza, Multicomponent toughened ceramic materials obtained by reaction sintering, J. Mater. Sci., Vol. 20, (1985), pp. 2011-2022

[16] W. Mista, J. Wrzyszcz, Rehydration of transition aluminas obtained by flash calcination of gibbsite, Thermochimica Acta., Vol. 331, (1999), pp. 67-72

[17] H. Belhouchet, M. Hamidouche, N. Bouaouadja, V. Garnier, G. Fantozzi, Elaboration and microstructural characterization of a mullite-zirconia composites obtained by reaction sintering, Ann. Chim. Sci. Mat., Vol. 32, N°6, (2007), pp. 605-614

[18] H. Belhouchet, M. Hamidouche, N. Bouaouadja, V. Garnier, G. Fantozzi, Elaboration and characterization of mullite-zirconia composites from gibbsite, boehmite and zircon, Ceram. Silikaty., Vol. 53, N°3, (2009), pp. 205-510

[19] T. Ebadzadeh, E. Ghasmi, Influence of starting materials on the reaction sintering of mullite-zirconia composites, J. Mater. Sci. Eng. A., Vol. 283, (2000), pp. 289-297

[20] Y. Shi, X. Huang and D. Yan, Fabrication of hot-pressed zircon ceramics: Mechanical properties and microstructure, Ceram. Inter., Vol. 23, (1997), pp. 457-462

[21] A. H. Heuer, N. Claussen, W. M. Kriven, M. Rhule, Stability of Tetragonal ZrO_2 Particles in Ceramic Matrices, J. Am. Ceram. Soc., Vol. 65, (1982), pp. 642-650

[22] Sci-Ke Zhao, Y. Huang, C-A. Wang, X-X. Huang, J-K. Guo, Sinterability of $ZrSiO_4$/α-Al_2O_3 mixed powders, Mater. Lett., Vol. 57, (2003), pp. 1716-1722